Microhydration of the Magnesium(II) Acetate Cation in the Gas Phase

Jana Paterová, Jan Heyda, Pavel Jungwirth,* Christopher J. Shaffer, Ágnes Révész, Emilie L. Zins, and Detlef Schröder*

Institute of Organic Chemistry and Biochemistry, Academy of Sciences of the Czech Republic, Flemingovo nám. 2, 166 10 Prague 6, Czech Republic

E-mail: Pavel.Jungwirth@uochb.cas.cz; Detlef.Schroeder@uochb.cas.cz

Received: ...

Proposed TOC graphic

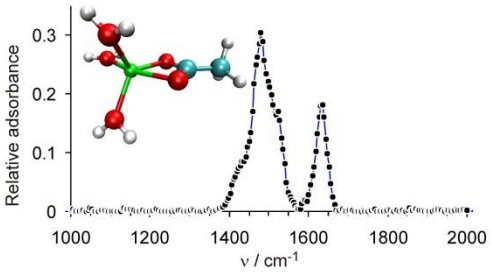

Abstract. Electrospray ionization of aqueous solutions of magnesium(II) acetate leads to microhydrated magnesium acetate cations of the type $[(CH_3COO)_{2m-1}Mg_m(H_2O)_n]^+$ with m = 1 - 4 and n = 0 - 4, which are characterized by mass spectrometry and, for the cluster with three water molecules, also by infrared multiphoton dissociation spectroscopy. Density functional theory is used to determine the energies of microhydration for the mononuclear species $[(CH_3COO)Mg(H_2O)_n]^+$ with n = 0 - 6 and the associated changes in molecular structure. While bidentate coordination of the acetato ligand is generally preferred, at higher values of n a switch to a monodentate coordination becomes energetically competitive.

Keywords: Electrospray ionization; density functional theory; ion association; magnesium acetate; microhydration

Introduction

Carboxylato ligands belong to an important family of binding partners in general coordination chemistry in general and play particular roles in bioinorganic chemistry in particular.[1] The alkaline earth ions Mg^{2+} and Ca^{2+} bind to the carboxylate groups of parvalbumins in muscles,[2] acetato bridges are a key motif of iron-containing methane monooxygenase,[3] and a switch between mono- and bidentate coordination (Scheme 1) in zinc enzymes has been referred to as "carboxylate shift".[4,5]

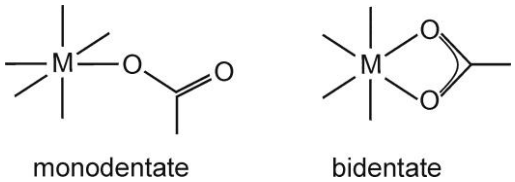

Scheme 1. Mono- and bidentate binding modes of an acetato ligand to a metal ion.

Our specific interest lies in the microhydration[6] of the corresponding $(CH_3COO)Mg^+$ "core" in the gas phase to form the corresponding $[(CH_3COO)Mg(H_2O)_n]^+$ complexes with a variable number of

* Corresponding author. Phone 00420 220 183 463 (DS).

water ligands *n*. The main objective is to probe the strength of the microhydration in the gas phase and its influence on the structure of the acetato ligand. To this end, we apply a combination of gas-phase experiments using electrospray ionization (ESI) mass spectrometry and quantum chemical calculations.[7] One of the long-term aims is to probe the existence of possible correlations between gas-phase results obtained using electrospray ionization and solution-phase data.[8,9]

Experimental and computational methods

Initial mass spectra were recorded with VG BioQ triple quadrupole mass spectrometer which has been described elsewhere.[10] The collision experiments were performed using a Finnigan LCQ Classic ion-trap mass spectrometer (IT-MS).[11] The ions of interest were generated by ESI of dilute aqueous solutions of magnesium(II) acetate. In brief, the LCQ bears a conventional ESI source consisting of the spray unit (typical flow rates between 5 and 30 μl/min., typical spray voltage 5 kV) with nitrogen as a sheath gas, followed by a heated transfer capillary (kept at 200 ºC), a set of lenses which determines the soft- or hardness of ionization by variation of the degree of collisional activation in the medium pressure regime,[12,13] two transfer octopoles, and a Paul ion-trap with ca. 10^{-3} mbar helium for ion storage and manipulation, including a variety of MS^n experiments.[14] For detection, the ions are ejected from the trap to an electron multiplier. Low-energy CID was performed by application of an excitation AC voltage to the end caps of the trap to induce collisions of the isolated ions with the helium buffer gas.[15] For a CID excitation period of 20 ms and a trapping parameter of $q_z = 0.25$, we have recently introduced an empirical calibration scheme which allows conversion of the experimental appearance energies (*AEs*) of the fragmentations to an absolute energy scale.[16] The observed isotope patterns confirm all ion assignments made in the following. In order to confirm the assignments made, the masses of the triple and pentuple ions[17] were further determined on a SYNAPT G2 mass spectrometer (WATERS, Manchester, UK) which has a standard mass resolution of $m/\Delta m \approx 20000$ (see Supplementary Information).

In addition, gas-phase infrared spectra of mass-selected $[(CH_3COO)Mg(H_2O)_3]^+$ was recorded with a Bruker Esquire 3000 IT-MS[18-20] mounted to a beamline of the free electron laser at CLIO (Centre Laser Infrarouge Orsay, France). The ion of interest was generated by ESI from aqueous solution as described above and transferred into the ion trap. After mass selection, infrared multi-photon dissociation (IRMPD) was induced by admittance of four pulses of IR-laser light to the ion trap, resulting in a total cycling time of about half a second. For each wavelength, 8 scans were averaged to one mass spectrum which was stored, the procedure was repeated 3 times before the wavelength was changed and the data again averaged, such that each data point in the IRMPD spectra consist of 32 scans. Further, all IRMPD spectra were recorded at least two times independently and the spectra shown are the averaged scans. In the 45 MeV range in which CLIO

was operated in these experiments, the IR light covers a spectral range from 1000 to 2000 cm^{-1}. Note that in this kind of action spectra, the assumption that the amount of ion fragmentation is proportional to the IR absorbance is not always justified due to the multiphotonic nature of IRMPD, and thus the major weight is put on the peak positions, rather than the peak heights in the IRMPD spectra.[21] Further, consideration of the water-binding energies detailed below as well as the photon energies in the range from 1000 to 2000 cm^{-1} implies that at least five IR photons are required to bring about fragmentation of $[(CH_3COO)Mg(H_2O)_3]^+$, which is fully consistent with the multi-photon character of IRMPD. Note however that the IRMPD involves the stepwise absorption of multiple photons, rather than being a genuine multiphoton process with simultaneous absorption.

The quantum chemical calculations were performed with density functional theory using the B3LYP functional[22] in conjunction with the aug-cc-pVDZ basis sets[23] implemented in the Gaussian 03 suite.[24] For all optimized structures, frequency analysis at the same level of theory was performed in order to assign them as genuine minima or transition structures on the potential-energy surface (PES) as well as to calculate zero-point vibrational energies (ZPVEs) and thermal corrections. The relative enthalpies and free enthalpies given below refer to a temperature of 298 K in the gaseous state; solvation, aggregation, etc. are deliberately not included, in order to match the present experimental conditions.

Table 1. Benchmarking of the B3LYP/aug-cc-pVDZ method for the $[(CH_3COO)Mg]^+$ ion in terms of the Mg-O distance (r_{MgO} in Å) and the heterolytic bond dissociation energy (electronic ΔE_{het} at 0 K in kJ mol^{-1}).[a]

Method	Basis set	r_{MgO}	ΔE_{het}
B3LYP	aug-cc-pVDZ	1.932	- 1585.2
B3LYP	aug-cc-pVTZ	1.923	- 1593.9
MP2	aug-cc-pVDZ	1.956	- 1539.0
MP2	aug-cc-pVTZ	1.940	- 1550.0
MP2	aug-cc-pVQZ	1.934	- 1554.3
MP2	CBS	-[b]	- 1556.1
CCSD(T)	aug-cc-pVDZ	1.953	- 1542.7

[a] Heterolytic dissociation into Mg^{2+} + CH_3COO^-. [b] Value extrapolated to the complete basis set (CBS) limit; no geometry optimization in the extrapolation.

The applicability of the B3LYP/aug-cc-pVDZ method was tested for the parent ion $[(CH_3COO)Mg]^+$ against MP2 with different basis sets and CCSD(T)/aug-cc-pVDZ. The data in Table 1 demonstrates that B3LYP/aug-cc-pVDZ performs reasonably well both in terms of geometry (Mg-O distance) and energetics (heterolytic dissociation into Mg^{2+} and CH_3COO^-). Additionally, we have performed benchmarks of B3LYP/aug-cc-pVDZ against MP2 for the binding energies of the most weakly bound H_2O molecule in clusters with $[(CH_3COO)Mg(H_2O)_n]^+$ with n = 1 - 6. Again, B3LYP/aug-cc-pVDZ performs very well for these systems with a pronounced

electrostatic bonding (Table 2). For these reason and since the CCSD(T) method becomes impractical for larger systems we employed the B3LYP approach as the main method throughout the present study. For determining the subtle balance between monodentate and bidentate structures of the microhydrated ion-pair we, however, use the more accurate MP2 energies.

Additionally, using the Amber program[25] we performed MD simulations of a single covalent ion pair of magnesium acetate (i.e. $[(CH_3COO)Mg]^+$) in bulk water at ambient conditions (300 K, 1 atm) to select representative sets of structures for *ab-initio* calculations of clusters containing magnesium acetate with 6 water molecules (see below). The system contained one acetate anion,[26] one Mg^{2+} dication,[26] and 353 SPC/E water molecules.[27] Three-dimensional periodic boundary conditions were applied and long-range electrostatic interactions beyond the non-bonded cutoff of 7.5 Å were accounted for using the particle mesh Ewald method[28] with a compensating background charge of -e. The Berendsen temperature (300 K) and pressure (1 atm) couplings were employed,[29] and all bonds containing hydrogens were constrained using the SHAKE algorithm.[30]

Table 2. Benchmarking of the B3LYP/aug-cc-pVDZ method in terms of the binding energies (electronic ΔE **at 0 K** in kJ mol^{-1}) of the most weakly bound water molecule in the microsolvated clusters $[(CH_3COO)Mg(H_2O)_n]^+$ with n = 1 - 6.

	B3LYP (aug-cc-pVDZ)	MP2 (aug-cc-pVDZ)	MP2 (aug-cc-pVTZ)
$[(CH_3COO)Mg(H_2O)]^+$	- 197.9	- 196.3	- 196.4
$[(CH_3COO)Mg(H_2O)_2]^+$	- 145.8	- 151.8	- 152.6
$[(CH_3COO)Mg(H_2O)_3]^+$	- 110.4	- 121.3	- 121.5
$[(CH_3COO)Mg(H_2O)_4]^+$	- 71.5	- 84.6	- 85.7
$[(CH_3COO)Mg(H_2O)_5]^+$	- 72.4	- 82.0	- 81.4
$[(CH_3COO)Mg(H_2O)_6]^+$	- 60.3	- 63.9	- 63.7

Due to the fact that magnesium acetate creates ion-pairs which are stable for tens of nanoseconds[26] two independent initial conditions were employed. A first simulation started from bidentate structure and enabled sampling of bidentate and monodentate configurations. Another simulation started from a distant separation of anion and cation and sampled solvent shared structures. Independent of the initial condition employed the system was first minimized with the method of steepest descent, then annealed (20 ps) and equilibrated (50 ps), before the production phase of the simulation (100 ns).

Ten geometries of $[(CH_3COO)Mg(H_2O)_6]^+$ were minimized for each of three cases under study (i.e., bidentate, monodentate, and solvent shared pair) at the B3LYP/aug-cc-pVDZ level. Ten initial structures were selected from the MD simulations with the ten closest water molecules to the oxygen atoms of carboxyl group. The eleventh initial structure was prepared by adding six water molecules to the $[(CH_3COO)Mg]^+$ core using chemical intuition.

Results and discussion

Electrospray ionization of a ca. 10^{-3} molar aqueous solution of magnesium(II) acetate gives rise to three series of mononuclear microhydrated ions (Table 3), i.e. $[(CH_3COO)Mg(H_2O)_n]^+$ (m/z = 83 + 18n for the leading isotope ^{24}Mg; n = 0 - 4), $[(CH_3COO)Mg(CH_3COOH)(H_2O)_n]^+$ (m/z = 143 + 18n; n = 0 - 3), and $[(CH_3COO)Mg(CH_3COOH)_2(H_2O)_n]^+$ (m/z = 203 + 18n; n = 0 - 2). The latter ions are likely formed via replacement of water ligands with traces of free acetic acid, whose presence is inherent to an aqueous solution of a salt composed from a weak acid and a weak base. In addition to the mononuclear species, a series of smaller cluster ions is observed which follow the general formula $[(CH_3COO)_{2m-1}Mg_m(H_2O)_n]^+$ with the largest members observed at m = 4 for the concentration chosen.[31] Similarly for these clusters, the exchange of water ligands by acetic acid also takes place. In negative-mode electrospray, the corresponding clusters of the type $[(CH_3COO)_{2m+1}Mg_m]^-$ (m = 1 - 7) are observed without any evidence for microhydration.[32] Because our interest is in the microhydration, we only pursue the cationic species, in particular the mononuclear complexes $[(CH_3COO)Mg(H_2O)_n]^+$.

Table 3. Experimental and calculated masses of selected cations in the ESI mass spectrum of an aqueous solution of magnesium(II) acetate (c = 10^{-3} mol l^{-1})[a] and their relative abundances under soft ionization conditions.

Species	m_{exp}[b]	m_{calc}	Δm[c]	I_{rel}[d]
$[(CH_3COO)Mg(H_2O)_2]^+$	119.0197	119.0195	0.2	3
$[(CH_3COO)Mg(H_2O)_3]^+$	137.0305	137.0301	0.4	16
$[(CH_3COO)Mg(H_2O)_4]^+$	155.0434	155.0406	2.8	2
$[(CH_3COO)Mg(CH_3COOH)(H_2O)]^+$	161.0293	161.0301	-0.7	13
$[(CH_3COO)Mg(CH_3COOH)(H_2O)_2]^+$	179.0427	179.0406	2.1	100
$[(CH_3COO)Mg(CH_3COOH)(H_2O)_3]^+$	197.0490	197.0512	-2.2	4
$[(CH_3COO)_3Mg_2(H_2O)]^+$	225.0086	225.0100	-1.4	1
$[(CH_3COO)_3Mg_2(H_2O)_2]^+$	261.0321	261.0311	1.0	12
$[(CH_3COO)_5Mg_3]^+$	367.0203	367.0217	-1.4	2
$[(CH_3COO)_7Mg_4]^+$	509.0329	509.0333	-1.1	<1

[a] The effective concentrations sampled in ESI are significantly larger, see ref. 31. [b] High resolution data taken on the SYNAPT G2 instrument. [c] Mass deviation in 10^{-3} amu. [d] Data taken on the VG BioQ instrument normalized to the largest peak (100).

In electrospray ionization, the number of solvent ligands coordinated to an ion of given composition and charge has a critical dependence on the potentials, the gas flows in the ion source, and the temperature of the transfer capillary separating the region with atmospheric pressure from the first stage of differential pumping.[12,13,33] Specifically, low potentials, low gas flows, and low temperatures favor large values of n, whereas elevated potentials accelerate the ions within the flowing gas leading to heating of the ionic species and thereby evaporation of solvent molecules and small values of n; likewise elevated gas flows or higher temperature favor solvent evaporation.

In comparing the different ions formed, it is instructive to consider the average hydration number n_{av}. For a hydrated cation $M(H_2O)_n^{z+}$, this formal parameter is calculated as $n_{av} = \Sigma(n_i \bullet I(n_i)) / \Sigma I(n_i)$, where $I(n)$ stands for the abundance of the core ion M^{z+} having n water ligands.[9d,34,35] Under soft ionization conditions, i.e. low temperatures and low potentials in ion transfer, multiply hydrated species prevail. With increasing temperature and/or voltages, successive evaporation of solvent molecules takes place concomitant with a continuous decrease of n_{av}. Multiple energetic collisions with nitrogen gas at further elevated potentials lead to the complete stripping of all solvent molecules ($n_{av} = 0$) and even subsequent fragmentations up to atomization.[36] Here, we have chosen reasonably soft, but not the most gentle conditions, in order to reach reasonable compromise between ion intensity, stability of the source, and microhydration.[37] Despite this variability, at a given setting of the ionization parameters, the relative values have been shown to provide insight about the water binding energies of the ions under study.[8,34,35,38] In this respect, no particular trends are observed for the cations formed upon ESI of $(CH_3COO)_2Mg_{aq}$. Specifically, $n_{av} = 2.94$ is found for the $[(CH_3COO)Mg(H_2O)_n]^+$ ions, $n_{av} = 1.92$ for $[(CH_3COO)Mg(CH_3COOH)(H_2O)_n]^+$, and $n_{av} = 0.90$ for $[(CH_3COO)Mg(CH_3COOH)_2(H_2O)_n]^+$. Adding the number of acetic acid ligands to these values, we arrive at a common value of 2.92 ± 0.02 for all three types of ions. In other words, the incoming acetic acid replaces only a single water ligand, suggesting that the free acid acts as a monodentate ligand in the acetato complexes. Assuming a bidentate acetato ligand, the value of about 3 leads to a total coordination number of five for the central magnesium atom. We note in passing that for the corresponding series of dinuclear clusters, i.e. the monocations $[(CH_3COO)_3Mg_2(H_2O)_n]^+$, $[(CH_3COO)_3Mg_2(CH_3COOH)(H_2O)_n]^+$, and $[(CH_3COO)_3Mg_2(CH_3COOH)_2(H_2O)_n]^+$, n_{av} amounts to 2.13, 1.03, and 0.05, respectively, which add to a common value of 2.07 ± 0.05 when acetic acid is included in the ligand count. Compared to the mononuclear species, the decreased coordination number of the dinuclear clusters is consistent with the intuitive assumption that the acetato groups act as bidendate ligands.[39]

Table 4. Experimental appearance energies (in kJ mol^{-1})[a] for the loss of water from the mononuclear $[(CH_3COO)Mg(H_2O)_n]^+$ ions (n = 1 - 3) and the dinuclear species $[(CH_3COO)_3Mg_2(H_2O)_n]^+$ (n = 1 ,2), respectively.

Species	*AE*
$[(CH_3COO)Mg(H_2O)]^+$[b]	160
$[(CH_3COO)Mg(H_2O)_2]^+$[b]	122
$[(CH_3COO)Mg(H_2O)_3]^+$	86
$[(CH_3COO)_3Mg_2(H_2O)]^+$[b]	124
$[(CH_3COO)_3Mg_2(H_2O)_2]^+$	98

[a] The experimental error of the appearance energy amounts to ± 20 %. For a detailed discussion, see ref. 16. [b] In the CID experiment with this ion, a significant amount of water uptake after the CID pulse prior to detection is observed.

As expected, the sequential water-binding energies of the microhydrated magnesium acetate ions, as derived from collision-induced dissociation (CID) experiments, continuously decrease with the increasing number of water ligands for both the mono- and dinuclear species (Table 4). Furthermore, the water-binding energy of the first water ligand to mononuclear $[(CH_3COO)Mg]^+$ exceeds that of the dinuclear species $[(CH_3COO)_3Mg_2]^+$, as expected.[9d,34,40] While observed experimentally, the tetraaquo complex $[(CH_3COO)Mg(H_2O)_4]^+$ could not be studied this way, because it looses a water ligand already in the course of the mass-selection process, indicating that the fourth water ligand is only weakly bound (see below).

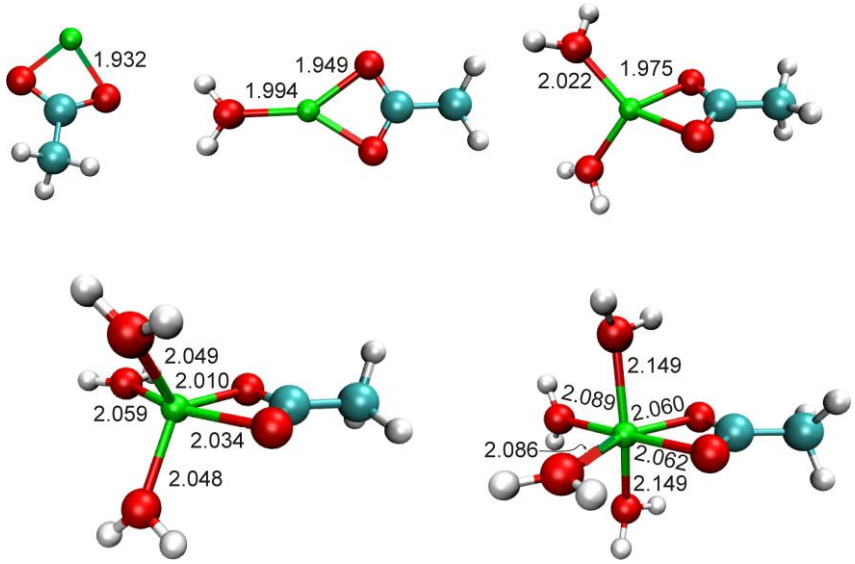

Figure 1. Optimized structures of the mononuclear $[(CH_3COO)Mg(H_2O)_n]^+$ ions up to n = 4 calculated using B3LYP/aug-cc-pVDZ with selected bond lengths given in Å.

The experimental results are complemented by a series of ab initio calculations. Figure 1 shows optimized structures of the microhydrated $[(CH_3COO)Mg(H_2O)_n]^+$ ions up to n = 4. In the core ion $[(CH_3COO)Mg(H_2O)_n]^+$, the acetato ligand is bidendate with identical bond lengths of r_{MgO} = 1.932 Å. The distances between the oxygen atoms of the acetate and the magnesium continuously increase with the number of water ligands, i.e. r_{MgO} = 1.949 Å for the monohydrate and r_{MgO} = 1.975 Å for n = 2, which both show symmetrical bidendate binding of the acetato ligand.[26,41] In the case of the trishydrated cation, the additional water ligand enters through the plane of the OCO unit, leading to a binding with two different bond lengths between the oxygen atoms of the acetate and the magnesium, r_{MgO} = 2.010 and 2.034 Å. Note that the larger bond length of the oxygen atom opposite to the water ligand in the OCO plane is an indication of the *trans*-effect in coordination chemistry.[42] Consistent with this interpretation, the binding of the acetato ligand is again quasi-symmetrical for n = 4, i.e. r_{MgO} = 2.060 and 2.062 Å, respectively; the small difference can be ascribed to an effect of the perpendicular conformations of the *trans*-standing water ligands. A similar effect is found for the next two water ligands, in that the binding of the acetato ligand is

again significantly unsymmetrical for n = 5, but almost symmetrical for n = 6. Other than a similar increase of r_{MgO} with increasing n, only two specific items necessitate elaboration as far as the water ligands are concerned. First, the changes in geometry between n = 3 and n = 4 are quite significant. In $[(CH_3COO)Mg(H_2O)_3]^+$, the three water ligands and the magnesium form an almost symmetrical pyramid opposed with a bidentate acetato ligand. In contrast, $[(CH_3COO)Mg(H_2O)_4]^+$ bears a quasi-octahedral structure with substantially enlarged Mg-O distances of the axial water ligands. Second, the Mg-O distances of the two other water ligands increase significantly, such that the average of all water ligands increases from $r_{MgO,av}$ = 2.052 Å for n = 3 to 2.158 Å for n = 4. This finding implies a weaker binding of the fourth water ligand compared to the smaller hydrates.

Table 5 summarizes the calculated water-binding energies of the $[(CH_3COO)Mg(H_2O)_n]^+$ ions up to n = 6. These results are consistent with experimental results in that the water-binding energies show a sharp drop between n = 3 and n = 4. This effect also plays into observation of the large abundance of n = 3 upon ESI-MS under soft conditions, and the low abundance of n = 4, for which the computed free energy for the loss of water approaches the range of thermal energy.

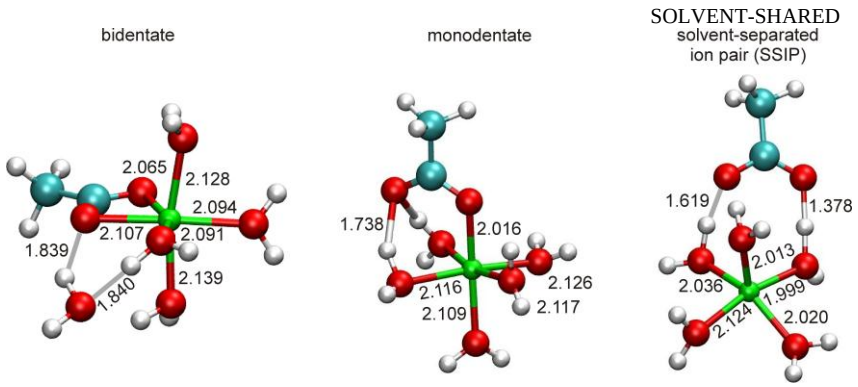

Figure 2. Optimized structures and relative energies of three conceptually different types of binding for the pentahydrate $[(CH_3COO)Mg(H_2O)_5]^+$ calculated using B3LYP/aug-cc-pVDZ.

An important aspect of the investigated clusters is that for clusters with up to 4 water molecules, the bidendate coordination of the acetato ligand is strongly preferred energetically. However, this preference steadily decreases upon adding water molecules, therefore, in transition from the quasi-octahedral $[(CH_3COO)Mg(H_2O)_4]^+$ to n = 5, one may expect that the fifth water molecule could replace one of the oxygen atoms of the acetato group leading to a monodentate situation. While the corresponding structure is a genuine minimum on the potential-energy surface, it is still higher in energy than the bidentate geometry (Figure 2 and Table 6). Based on MP2 relative energies, corrected for ZPVEs from the B3LYP level calculations, we predict the population of monodentate structure to be about 9 % of that of the bidentate at ambient conditions (Table 6). In the cluster with 6 water molecules, the situation reverses and the monodentate structure becomes the global minimum, being almost three times more populated than the bidentate geometry (Figure 3). We note in passing that comparing B3LYP to MP2 the former appears to favor the bidentate situation.[43]

Irrespective of the thus somewhat limited certainty of the theoretical predictions, the observed coexistence of these two structures is in accord with experimental and computational observations in bulk magnesium acetate solutions, where both monodentate and bidentate geometries were observed.[25] Note, however, that unlike in the aqueous bulk[25] the population of solvent-shared structures is still very low in the investigated clusters due to the small number of available water molecules (Table 6).

SOLVENT-SHARED

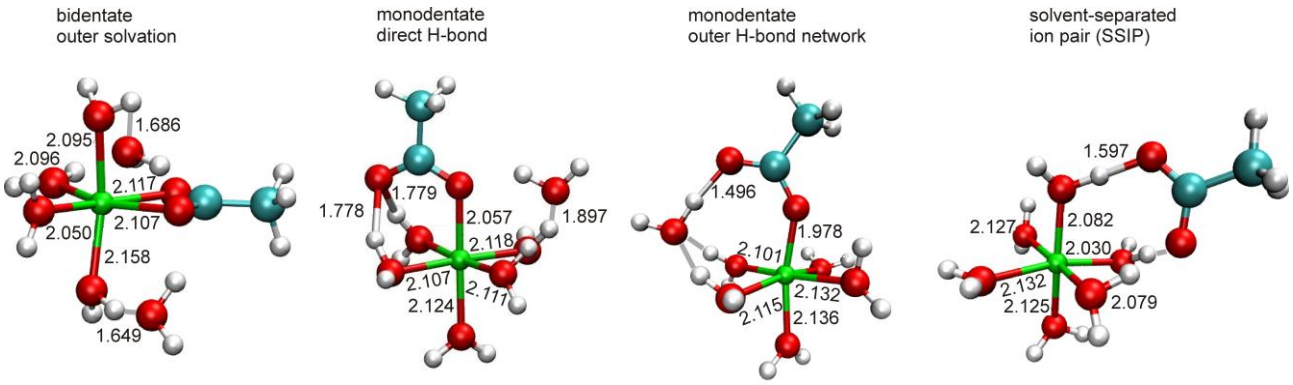

Figure 3. Optimized structures and relative energies of three conceptually different types of binding for the hexahydrate $[(CH_3COO)Mg(H_2O)_6]^+$ calculated using B3LYP/aug-cc-pVDZ.

Table 5. Sequential water-binding energies (in kJ mol^{-1})[a] of the mononuclear $[(CH_3COO)Mg(H_2O)_n]^+$ ions up to n = 6 calculated using B3LYP/aug-cc-pVDZ.

Species	ΔH_{298}	ΔG_{298}	$\Delta\Delta G$[b]
$[(CH_3COO)Mg(H_2O)]^+$	190	154	55
$[(CH_3COO)Mg(H_2O)_2]^+$	138	99	36
$[(CH_3COO)Mg(H_2O)_3]^+$	104	63	44
$[(CH_3COO)Mg(H_2O)_4]^+$	64	19	5
$[(CH_3COO)Mg(H_2O)_5]^+$	64	14	-6
$[(CH_3COO)Mg(H_2O)_6]^+$	55	20	-[b]

[a] Adiabatic values, i.e. fully relaxed geometries. [b] Drop of the water-binding free enthalpies between n and n+1; no entry for n = 6 because the next cluster with n = 7 was not included in the computational study.

Table 6. Relative energies and the corresponding thermal populations (x_i) of bidentate, monodentate, and solvent-shared geometries of $[(CH_3COO)Mg(H_2O)_n]^+$ in clusters of n = 5 or 6.

	n = 5		n = 6	
	E_{rel} (kJ mol^{-1}) B3LYP/MP2	x_i (based on MP2 energy and B3LYP ZPVEs)	E_{rel} (kJ mol^{-1}) B3LYP/MP2	x_i (based on MP2 energy and B3LYP ZPVEs)
bidentate	0.0/0.0	0.92	0.0/0.0	0.28
monodentate	8.6/7.6	0.08	-0.7/-7.6	0.72
monodentate outer H-bond network	-	-	18.3/20.1	2.9×10^{-4}
solvent shared	56.8/69.6	1.6×10^{-11}	37.6/39.0	5.3×10^{-7}

Highlighting these studies, one representative of the microhydrated magnesium acetate ions was additionally characterized by infrared spectroscopy in the gas phase. To this end, the mass-selected

ion $[(CH_3COO)Mg(H_2O)_3]^+$ generated via ESI was stored in an ion trap and allowed to interact with infrared radiation from the tunable IR laser CLIO (Orsay, France). If the ions under study absorb the intense IR light, fragmentation occurs which provides the observable property in this kind of spectroscopy. Because the water binding energies exceed the energy of single IR photons, sequential absorption of several photons is required, and the method is accordingly referred to as infrared multiphoton-dissociation (IRMPD).[44] The IRMPD spectrum shows a broad, structured feature at about 1500 cm^{-1} and a second sharper band at 1630 cm^{-1}, respectively (Figure 4). The former is assigned to overlapping modes associated with CH_2 bending and symmetric as well as asymmetric C-O stretching. In contrast, the carbonyl stretch of a monodentate acetato ligand should occur at larger wavenumbers.[5,41,45] The second band slightly above 1600 cm^{-1} is due to the bending modes of water and is characteristic for microhydrated metal cations.[46] Comparison with the calculated spectrum (see blue bars in Figure 4) shows reasonable agreement with the bidendate structure shown in Figure 1, whereas other conceivable isomers can safely be excluded (for details, see the Supplementary Information). Similar IRMPD experiments with the smaller hydrates $[(CH_3COO)Mg(H_2O)]^+$ and $[(CH_3COO)Mg(H_2O)_2]^+$ were impossible in the ion trap, due to a rapid addition of water present in the background such that the IR patterns would always overlap with that of $[(CH_3COO)Mg(H_2O)_3]^+$.

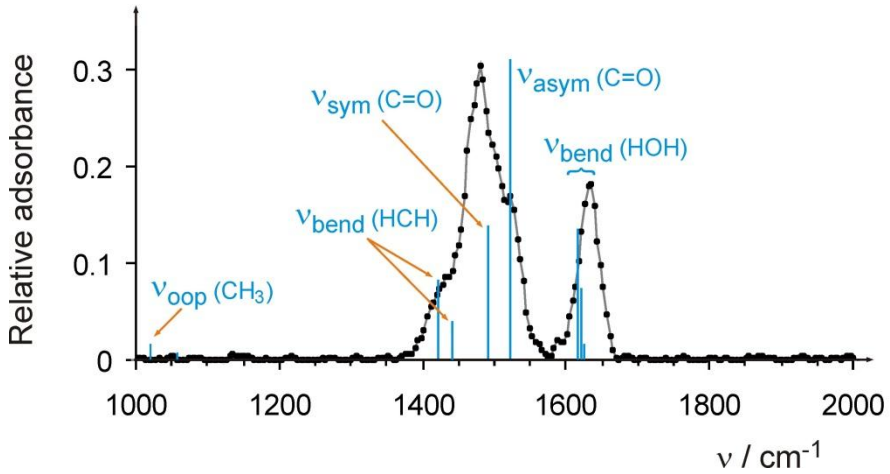

Figure 4. IRMPD spectrum of the mass-selected $[(CH_3COO)Mg(H_2O)_3]^+$ cation in the spectral range from 1000 to 2000 cm^{-1}. The computed IR transitions are indicated as blue bars.

Conclusions

The microhydration of magnesium acetate ions $[(CH_3COO)Mg(H_2O)_n]^+$ in the gas phase is probed by experimental and computational means. The experiments indicate a significant decrease of the water-binding energies between $[(CH_3COO)Mg(H_2O)_3]^+$ and $[(CH_3COO)Mg(H_2O)_4]^+$, which is fully confirmed by the theoretical results. With regard to the binding of the acetato ligand, a bidentate coordination is largely preferred. Moreover, it turns out that even for larger values of *n*, the bidentate coordination of the acetato ligand remains competitive in the equilibrium geometry.

Instead, after formation of a quasi-octahedral coordination environment of the metal, the addition of water ligands form an outer solvation shell stabilized by a network of hydrogen bonds.

Acknowledgments. This work was supported by the Academy of Sciences of the Czech Republic (Z40550506), the European Research Council (AdG HORIZOMS), and the Grant Agency of the Czech Republic (203/08/1487). ELZ, AR, and DS thank the entire team of CLIO for support in the IRMPD measurements (project IC 021-10). PJ thanks for support to the Academy of Sciences of the Czech Republic (Praemium Academie) and the Grant Agency of the Czech Republic (grant 203/08/0114), and JP acknowledges support from the International Max-Planck Research School.

Supplementary information available. The infrared spectra of additional structures of $[(CH_3COO)Mg(H_2O)_n]^+$ and their discussion in terms of the IRPMD experiments are available free of charge via the Internet at http://pubs.acs.org.

References

(1) Kaim, W.; Schwederski, B. Bioinorganic Chemistry: Inorganic Elements in the Chemistry of Life, Wiley, New York, 1994

(2) Haiech, J.; Derancourt, J.; Pechère, J. F.; Demaille, J. G. *Biochemistry* **1979**, *18*, 2752.

(3) Rosenzweig, A. C.; Frederick, C. A.; Lippard, S. J.; Nordlund, R. *Nature* **1993**, *366*, 537.

(4) Sousa, S. F.; Fernandes, P. A.; Ramos, M. J. *J. Am. Chem. Soc.* **2007**, *129*, 1378, and references therein.

(5) For a recent gas-phase example of the carboxylate shift, see: Ducháčková, L.; Schröder, D.; Roithová, J. *Inorg. Chem.*, in press (doi: 10.1021/ic2002767).

(6) For a review of microhydrated ions, see: Beyer, M. K. *Mass Spectrom. Rev.* **2007**, *26*. 517.

(7) For a similar earlier study of microhydrate magnesium(II) nitrate cations, see: Jagoda-Cwiklik, B.; Jungwirth, P.; Rulíšek, L.; Milko, P.; Roithová, J.; Lemaire, J.; Maitre, P.; Ortega, J. M.; Schröder, D. *ChemPhysChem* **2007**, *8*, 1629.

(8) Di Marco, V. B.; Bombi, G. G. *Mass Spectrom. Rev.* **2006**, *25*, 347.

(9) For attempts towards quantitative correlations, see: (a) Cheng, J.; Hoffmann, M. R.; Colussi, A. J. *J. Phys. Chem. B* **2008**, *112*, 7157. (b) Walther, C.; Fuss, M.; Büchner, S. *Radiochim. Acta* **2008**, *96*, 411. (c) Urabe, T.; Tsugoshi, T.; Tanaka, M. *J. Mass. Spectrom.* **2009**, *44*, 193. (d) Tsierkezos, N. G.; Roithová, J.; Schröder, D.; Ončák, M.; Slavíček, P. *Inorg. Chem.* **2009**, *48*, 6287. (e) Psillakis, E.; Cheng, J.; Hoffmann, M. R.; Colussi, A. J. *J. Phys. Chem. A* **2009**, *113*, 8826. (f) Koszinowski, K. *J. Am. Chem. Soc.* **2010**, *132*, 6032. (g) Enami, S.; Hoffmann, M. R.; Colussi, A. J. *J. Phys. Chem. Lett.* **2010**, *1*, 1595. (h) Agrawal, D.; Schröder, D.; Sales, D. A.; Lloyd-Jones G. C. *Organometallics* **2010**, *29*, 3979. (i) Ducháčková, L.; Roithová, J.; Milko, P.; Žabka, J.; Tsierkezos, N.; Schröder, D. *Inorg. Chem.* **2011**, *50*, 771. See also: (j) Cheng, Z. L.; Siu, K. W. M.; Guevremont, R.; Berman, S. S. *J. Am. Soc. Mass Spectrom.* **1992**, 3, 281. (k) Šadech, V.; Schröder, D.; Tsierkezos, N. G. *Int. J. Mass Spectrom.*, in press (doi: 10.1016/j.ijms.2011.02.014).

(10) Schröder, D.; Weiske, T.; Schwarz H.*Int. J. Mass Spectrom.* **2002**, *219*, 729.

(11) Tintaru, A.; Roithová, J.; Schröder, D.; Charles, L.; Jušinski, I.; Glasovac, Z.; Eckert-Maksić, M. *J. Phys. Chem.* **2008**, *112*, 12097.

(12) Cech, N. B.; Enke, C. G. *Mass Spectrom. Rev.* **2001**, *20*, 362.

(13) Schröder, D.; Weiske, T.; Schwarz, H. *Int. J. Mass Spectrom.* **2002**, *219*, 729.

(14) O'Hair, R. A. J. *Chem. Commun.* **2006**, 1469.

(15) (a) Tsierkezos, N. G.; Buchta, M.; Holý, P.; Schröder, D. *Rap. Commun. Mass Spectrom.* **2009**, *23*, 1550. (b) Agrawal, D.; Zins, E. L.; Schröder, D. *Chem. Asian J.* **2010**, *5*, 1667.

(16) (a) Révész, Á.; Milko, P.; Žabka, J.; Schröder, D.; Roithová, J. *J. Mass Spectrom.* **2010**, *45*, 1246. (b) Zins, E. L.; Pepe, C.; Schröder, D. *J. Mass Spectrom.* **2010**, *45*, 1253. (c) Remeš, M.; Roithová, J.; Schröder, D.; Cope, E. D.; Perera, C.; Senadheera, S. N.; Stensrud, K.; Ma, C.-C.; Givens, R. S. *J. Org. Chem.*, in press (doi: 10.1021/jo1025223).

(17) These terms are used to characterize higher-order aggregates of ions in solution. In the case of aqueous sodium chloride, for example, Na_{aq}^+ and Cl_{aq}^- are the free ions, $[Na^+ \bullet Cl^-]_{aq}$ is an ion pair, $[Na^+ \bullet Cl^- \bullet Na^+]_{aq}$ and $[Cl^- \bullet Na^+ \bullet Cl^-]_{aq}$ are triple ions etc. See: Marcus, Y.; Hefter, G. *Chem. Rev.* **2006**, *106*, 4585.

(18) Mac Aleese, L.; Simon, A.; McMahon, T. B.; Ortega, J. M.; Scuderi, D.; Lemaire, J.; Maitre, P. *Int. J. Mass Spectrom.* **2006**, *249*, 14.

(19) Chiavarino, B.; Crestoni, M. E.; Fornarini, S.; Lanucara, F.; Lemaire, J.; Maitre, P. *Angew. Chem. Int. Ed.* **2007**, *46*, 1995.

(20) Simon, A.; Aleese, L.; Maitre, P.; Lemaire, J.; McMahon, T. B. *J. Am. Chem. Soc.* **2006**, *129*, 2829.

(21) (a) Schröder, D. Schwarz, H. Milko, P. Roithová, J. *J. Phys. Chem. A* **2006**, *110*, 8346. (b) Schröder, D.; Ducháčková, L.; Jušinski, I.; Eckert-Maksić, M.; Heyda, J.; Tůma, L.; Jungwirth, P. *Chem. Phys. Lett.* **2010**, *490*, 14. (c) Jiang, L.; Wende, T.; Bergmann, R.; Meijer, G.; Asmis, K. R. *J. Am. Chem. Soc.* **2010**, *132*, 7398.

(22) (a) Becke, A. D. *J. Chem. Phys.* **1993**, *98*, 5648. (b) Vosko, S. H.; Wilk, L.; Nusair, M. *Can. J. Phys.* **1980**, *58*, 1200. (c) Lee, C.; Yang, W.; Parr, R. G. *Phys. Rev. B* **1988**, *37*, 785. (d) Miehlich, B.; Savin, A.; Stoll, H.; Preuss, H. *Chem. Phys. Lett.* **1989**, *157*, 200.

(23) Dolg, M.; Wedig, U.; Stoll, H.; Preuss, H. *J. Chem. Phys.* **1987**, *86*, 866.

(24) Gaussian 03, Revision C.02, Gaussian, Inc., Wallingford CT, 2004.

(25) Case, D. A. D., T. A.; Cheatham, III, T. E; Simmerling, C. L.; Wang, J.; Duke, R. E.; Luo, R.; Crowley, M.; Walker, R. C.; Zhang, W.; Merz, K. M.;Wang, B.; Hayik, S.; Roitberg, A.; Seabra, G.; Kolossvary, I.;Wong, K. F.; Paesani, F.; Vanicek, J.;Wu, X.; Brozell, S. R.; Steinbrecher, T.; Gohlke, H.; Yang, L.; Tan, C.; Mongan, J.; Hornak, V.; Cui, G.; Mathews, D. H.; Seetin, M. G.; Sagui, C.; Babin, V.; Kollman, P. A. Amber 10; Amber 10, University of California, San Francisco, 2008.

(26) Wahab, A.; Mahiuddin, S.; Hefter, G.; Kunz, W.; Minofar, B.; Jungwirth, P. *J. Phys. Chem. B* **2005**, *109*, 24108.

(27) Berendsen, H. J. C.; Grigera, J. R.; Straatsma, T. P. *J. Phys. Chem.* **1987**, *91*, 6269.

(28) Essmann, U.; Perera, L.; Berkowitz, M. L.; Darden, T.; Lee, H.; Pedersen, L. G. *J. Chem. Phys.* **1995**, *103*, 8577.

(29) Berendsen, H. J. C.; Postma, J. P. M.; Vangunsteren, W. F.; Dinola, A.; Haak, J. R. *J. Chem. Phys.* **1984**, *81*, 3684.

(30) Ryckaert, J. P.; Ciccotti, G.; Berendsen, H. J. C. *J. Comp. Phys.* **1977**, *23*, 327.

(31) To avoid misunderstanding of the cluster ion abundances, it is important to point out that the effective concentrations sampled in ESI are significantly larger than those of the solutions fed to the ESI source (see refs. 9d and 9h).

(32) See also: Jacob, A. P.; James, P. F.; O'Hair, R. A. J. *Int. J. Mass Spectrom.* **2006**, *255*, 45.

(33) For more detailed case studies, see: (a) Schröder, D.; Holthausen, M. C.; Schwarz, H. *J. Phys. Chem. B* **2004**, *108*, 14407. (b) Trage, C.; Diefenbach, M.; Schröder, D.; Schwarz, H. *Chem. Eur. J.* **2006**, *12*, 2454.

(34) Schröder, D.; de Jong, K. P.; Roithová, J. *Eur. J. Inorg. Chem.* **2009**, 2121.

(35) Tsierkezos, N. G.; Roithová, J.; Schröder, D.; Molinou, I. E.; Schwarz H. *J. Phys. Chem. B* **2008**, *112*, 4365.

(36) For related examples for desolvation and subsequent fragmentation of contact-ion pairs produced in ESI, see: (a) Schröder, D.; Roithová, J. *Angew. Chem. Int. Ed.* **2006**, *45*, 5705. (b) Roithová, J.; Schröder, D. *J. Am. Chem. Soc.* **2007**, *129*, 15311. (c) Schröder, D.; Roithová, J.; Alikhani, E.; Kwapien, K.; Sauer, J. *Chem. Eur. J.* **2010**, *16*, 4110. (d) Ref. 34.

(37) The actual settings of the LCQ were as follows: capillary voltage, -10 V; tube lens offset, -10 V; capillary temperature 200 ^{o}C. Note, however, that these settings only apply to the instrument used here and other ESI sources may have different values as well as parameters. Moreover, when working with mmolar salt solutions a significant deposition of solid material takes place within a day, which may affect these parameters and require adjustment depending upon the actual contamination of the source. Irrespective of these variations, the principal settings and phenomena of soft versus hard ionization in the ESI source remain the same.

(38) In this context we note that Williams and coworkers have used the degree of hydration of gaseous ions to derive a strategy for experimental nanocalorimetry in the gas phase, see: Donald, W. A.; Leib, R. D.; O'Brien, J. T.; Williams, E. R. *Chem. Eur. J.* **2009**, *15*, 5926. (b) Donald, W. A.; Leib, R. D.; Demireva, O'Brien, J. T.; Prell, J. S.; Williams, E. R. *J. Am. Chem. Soc.* **2009**, *131*, 13328. (c) Donald, W. A.; Williams, E. R. *J. Am. Soc. Mass Spectrom.* **2010**, *21*, 615. (d) Donald, W. A.; Demireva, M.; Leib, R. D.; Aiken, M. J.; Williams, E. R. *J. Am. Chem. Soc.* **2010**, *132*, 4633.

(39) A reviewer suggested a comparison of the water-binding energies in $[(CH_3COO)Mg(H_2O)_n]^+$ with those in the microhydrated $[Mg(H_2O)_n]^{2+}$ dications. Due to the difference in the real Coubomb charges, such a comparison is not too much insightful, because the sequential water-binding energies of Mg^{2+} are more than two times larger than those of the corresponding MgX^+ monocations (X = monovalent counterion); for an extensive treatment of $[Mg(H_2O)_n]^{2+}$ up to n = 9, see: Adrian-Scotto, M.; Mallet, G.; Vasilescu, D. *J. Mol. Struct.* **2005**, *728*, 231.

(40) Ončák, M.; Schröder, D.; Slavíček, P. *J. Comp. Chem.* **2010**, *31*, 2294.

(41) For the co-existence of mono- and bidendate carboxylato groups in gaseous uranyl complexes, see: Groenewold, G. S.; De Jong, W.; Oomes, J.; Van Stipdonk, M. J. *J. Am. Soc. Mass Spectrom.* **2010**, *21*, 719.

(42) Kauffmann, G. B. *J. Chem. Educ.* **1977**, *54*, 86.

(43) For a similar discrepancy between B3LYP and DFT in microhydrated cations, see: Cooper, T. E.; O'Brien, J. T.; Williams, E. R.; Armentrout, P. B. *J. Phys. Chem. A* **2010**, *114*, 12646.

(44) Dopfer, O. *J. Phys. Org. Chem.* **2006**, *19*, 540. (b) Polfer, N. C.; Oomens, J. *Phys. Chem. Chem. Phys.* **2007**, *9*, 3804. (c) Asmis, K. R.; Sauer, J. *Mass Spectrom. Rev.* **2007**, *26*, 542. (d) MacAleese, L.; Maitre, P. *Mass Spectrom. Rev.* **2007**, *26*, 583.

(45) Ducháčková, L., Steinmetz, V.; Lemaire, J.; Roithova, J. *Inorg. Chem.* **2010**, *49*, 8897.

(46) (a) Ref. 7. (b) Sinha, R. K.; Nicol, E.; Steinmetz, V.; Maitre, P. *J. Am. Chem. Soc. Mass Spectrom.* **2010**, *21*, 758. (c) Schröder, D.; Ducháčková, L.; Tarábek, J.; Karwowska, M.; Fijalkowski, K.; Ončák, M.; Slavíček, P. *J. Am. Chem. Soc.* **2011**, *133*. 2444.